Aggregate Harmonic Fingerprint Models of PV Inverters. Part 2: Operation of Parallel-Connected Units

S. Müller and J. Meyer
TU Dresden
Dresden, Germany

J. Myrzik
TU Dortmund
Dortmund, Germany

R. Langella and A. Testa
The University of Campania
Aversa, Italy

X. Xu, A. Collin, S. Djokic
The University of Edinburgh
Edinburgh, Scotland, UK

Abstract—**This paper is the second part of a two-part series on the development of aggregate frequency domain models (FDMs) of photovoltaic inverters (PVIs). The first-part paper presents measurement-based harmonic fingerprint models (HFMs) of individual PVIs, which require a large number of tests, in order to accurately represent power-dependent changes of PVIs harmonic characteristics. Part 1 paper also presents two suitable modifications of harmonic admittance matrices (HAMs), which allow for accurate representation of PVIs harmonic emission at different operating powers with significantly reduced number of required measurements. This paper evaluates operation of parallel-connected PVI units, investigating whether the correct aggregate HFM can be obtained from their individual HFMs, by summing-up the corresponding HAM elements. The paper compares the results for the aggregate HFMs obtained using individual HFMs from measurement-based and two modified HAM approaches, which are illustrated using an example of two parallel-connected PVIs. The presented HFM-based aggregation approach is specifically aimed for the analysis of networks with a large number of PVIs operating at different powers, as it allows for accurate and computationally efficient determination of their aggregate models and subsequent evaluation of their aggregate impact and effects on the grid and other connected equipment.**

Index Terms—**Frequency-domain, harmonic fingerprint model, harmonics, photovoltaic inverter, power quality.**

I. INTRODUCTION

This paper is the second part of a two-part series on the development of aggregate frequency domain models (FDMs) of photovoltaic inverters (PVIs). The main motivation for this work, as discussed in Part 1 paper [1], is a strong increase of the numbers of various types of PVIs over the recent years, which is anticipated to continue, if not to grow further, in the future. For example, the total installed PV capacity in the UK exhibited an extraordinary increase from around 30 MW in 2010, to around 12.6 GW at the end of 2017, of which around 54% (6.8 GW) are PV installations with rated power, P_{rated}, less than 5 MW and around 20% (2.5 GW) are highly dispersed small PVI units with P_{rated} less than 4 kW, typically connected to residential low voltage (LV) networks, [2].

In order to evaluate aggregate impact and effects of a large number of PV inverters in LV and medium voltage networks, the accurate models of PVIs are required, capable of correctly representing their harmonic emission characteristics under the entire range of operating powers and for different voltage supply conditions. However, the analysis of harmonic interactions between the individual PVIs, between the PVIs and supplying grid and between the PVIs and other connected equipment is a complex task, as it involves modelling of a large number of nonlinear devices under non-sinusoidal voltage supply conditions. Essentially, this eliminates the use of time-domain (or component-based) models from the analysis, due to model complexity and required computational times, but also due to the required knowledge on circuit topologies and control algorithms of modelled equipment.

An alternative to time-domain modeling approaches for evaluating harmonic emission is based on the use of measurement-based frequency domain models (FDMs), as they are less computationally intensive and do not require exact knowledge of the circuits and controls, what make them more suitable for the implementation in large-scale network studies. However, measurement-based FDMs require significant number of tests under carefully controlled test conditions, with further increase of required measurements in case of PVIs, as they usually exhibit strong power-dependent changes of harmonic characteristics. This is discussed in detail in Part 1 paper, where measurement-based harmonic fingerprint models (HFMs of three individual PVIs are presented, together with a novel approach, in which two suitable modifications of the related harmonic admittance matrices (HAMs) are proposed. The proposed HFMs use only one "reference HAM", which is multiplied by two coefficients calculated from the power-dependent changes of PVIs total subgroup current harmonic distortion, $THDS_I$. This results in a much simpler HFM, capable of accurately representing harmonic emission of PVIs at different operating powers with significantly reduced number of measurements.

This Part 2 paper provides further analysis and evaluation of operation of parallel-connected PVI units, investigating whether the correct aggregate HFM can be obtained from their individual HFMs, by summing-up the corresponding HAM elements. The paper compares the results for the aggregate HFMs obtained using individual HFMs from measurement-based and two proposed approaches with modified HAMs, which are illustrated using an example of two parallel-connected PVIs that are also analysed in Part 1 paper.

II. METHODOLOGY FOR BUILDING AGGREGATE HFMs

The main aim of this paper is to answer the following question: If individual HFMs are available for two or more parallel-connected power electronic devices, how accurate is an aggregate HFM obtained by summing-up corresponding HAM elements from their individual HFMs. The analysis is illustrated using an example of two parallel-connected PVIs operating at same or different powers, where summing (i.e. superposition) of HAM elements of individual HFMs is performed for four different types of individual HFMs (two are obtained in measurements and two are based on the modifications presented in Part 1 paper). These four sets of aggregate HFM-results are compared with the aggregate HFM obtained in direct measurements with two PVIs operating together, which is used as a reference model for the validation.

A. Measurement-Based Aggregate HFMs

A measurement-based aggregate HFM of two or more parallel-connected devices can be obtained in the same way as their individual HFMs. In the considered case of two parallel-connected PVIs, the same experimental set-up described and used in Part 1 paper for obtaining their individual measurement-based HFMs is also used to obtain their measurement-based aggregate HFM, with only one significant difference: two PV emulators are used and connected to two different PVIs, in order to adjust selected combinations of their operating powers. Furthermore, both PVIs are connected in parallel to a controllable three-phase power source, as one of the two PVIs is a three-phase unit. The basic experimental setup with marked relevant voltages and currents is illustrated in Fig. 1, while further details can be found in [3]-[5].
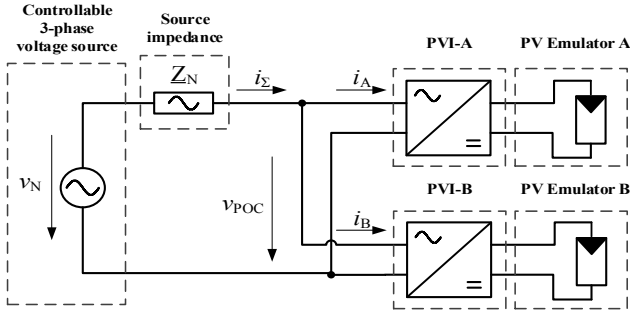
Fig. 1. Measurement setup

The two tested PVIs, marked as "PVI-A" and "PVI-B" in accordance to the notation used in Part 1 paper, are measured when operating individually and when operating in parallel, using the same test procedure described in Part 1 paper (regarding considered harmonic orders, adjusted operating powers, rms voltage magnitudes, etc.). Based on these measurements, the corresponding individual HFMs, with related HAMs, are obtained for PVI-A operating in the range from 100% of P_{rated} down to 10% of P_{rated} with a step of 10% of P_{rated} and for PVI-B from 50% to 5% of P_{rated}, with a 5% step, as well as variations of rms voltage magnitudes in the range from 0.9 pu to 1.1 pu.

Regarding the measurements of the two parallel-connected PVIs, the tested combinations of operating powers of PVI-A and PVI-B connected together are listed in Table I.

TABLE I. TESTED OPERATING POWERS FOR PARALLEL-CONNECTED PVIs

Case Identifier (P1&P2)	Operating Power (in % of P_{rated})	
	PVI-A (P1)	PVI-B (P2)
Case 10&10	10 %	10 %
Case 10&50	10 %	50 %
Case 50&10	50 %	10 %
Case 50&50	50 %	50 %

In order to provide a clear distinction based on notation applied in Part 1 paper, the *measurement-based individual* HFMs and corresponding HAM elements, obtained for PVI-A and PVI-B operating at specific powers P1 and P2, are denoted as "M1": $HFM_{M1\_PVI-A}(P1)$, $HAM_{\%\_M1\_PVI-A}(P1)$ and $\underline{Y}^{h,H}_{\%\_M1\_PVI-A}(P1)$ for PVI-A, and $HFM_{M1\_PVI-B}(P2)$, $HAM_{\%\_M1\_PVI-B}(P2)$ and $\underline{Y}^{h,H}_{\%M1_{PVI}-B}(P2)$ for PVI-B.

The *measurement-based aggregate* HFMs and corresponding HAM elements are marked with the additional subscript "Agg", corresponding to two following types of *measurement based aggregate* HFMs obtained by:

1. Direct measurements of parallel-connected PVI-A and PVI-B, operating at powers P1 and P2, denoted as "Ma" values: $HFM_{Agg\_Ma}(P1\&P2)$, $HAM_{\%\_Agg\_Ma}(P1\&P2)$ and $\underline{Y}^{h,H}_{\%\_Agg\_Ma}(P1\&P2)$, and

2. Summing-up Y-elements of two individual measurement-based HFMs for PVI-A and PVI-B, operating at powers P1 and P2, denoted as "M1" values: $HFM_{Agg\_M1}(P1\&P2)$, $HAM_{\%\_Agg\_M1}(P1\&P2)$ and $\underline{Y}^{h,H}_{\%\_Agg\_M1}(P1\&P2)$.

The calculation (summing-up) of $HAM_{\%\_Agg\_M1}(P1\&P2)$ elements from $HAM_{\%\_M1\_PVI-A}(P1)$ and $HAM_{\%\_M1\_PVI-B}(P2)$ elements is performed using:

$$\underline{Y}^{h,H}_{\%_{Agg\_M1}}(P1\&P2)\frac{\bar{I}^1_{Tot}(P1\&P2)}{\bar{V}^1} =$$
$$= \underline{Y}^{h,H}_{\%\_M1\_PVI-A}(P1)\frac{\bar{I}^1_{PV-A}(P1)}{\bar{V}^1} + \underline{Y}^{h,H}_{\%\_M1\_PVI-B}(P2)\frac{\bar{I}^1_{PV-B}(P2)}{\bar{V}^1} \quad (1)$$

where normalized values are obtained from absolute values using the corresponding fundamental input ac currents, $\bar{I}^1_{PVI-A}(P1)$, for PVI-A at power P1, $\bar{I}^1_{PVI-B}(P2)$, for PVI-B at power P2, $\bar{I}^1_{Tot}(P1\&P2)$, for PVI-A and PVI-B connected in parallel and operating at P1 and P2, respectively.

B. Aggregate HFMs Based on Two HAM modifications

The two HAM modifications presented in Part 1 paper allow to obtain two corresponding HFMs for individual PVIs with a significant reduction of required measurements, [1]. Both modifications use only one "reference HAM", multiplied by two coefficients calculated from power-dependent changes of PVIs total subgroup current harmonic distortion, $THDS_I$. This simplifies representation of power-dependent changes of PVIs harmonic characteristics, as the two related coefficients can be either prepared in advance and used as a "look-up table" (the first modification), or calculated from the actual $THDS_I$ value for a PVI operating at specific power and under specific voltage supply condition (the second modification). In that way, two proposed modifications allow for a simple but correct representation of PVIs harmonic characteristics for the entire range of their operating powers and for different voltage supply conditions, which is crucial for evaluating aggregate impact of a large number of PVIs.

Following the same notation applied in Part 1 paper, the two *modification-based individual* HFMs and corresponding HAM elements for PVI-A and PVI-B operating at powers P1 and P2 are denoted as "M2" and "M3" values, i.e. as: $HFM_{M2\_PVI-A}(P1)$, $HAM_{\%\_M2\_PVI-A}(P1)$ and $\underline{Y}_{\%\_M2\_PVI-A}^{h,H}(P1)$, and also $HFM_{M3\_PVI-A}(P1)$, $HAM_{\%\_M3\_PVI-A}(P1)$ and $\underline{Y}_{M3_{PVI-A}}^{h,H}(P1)$ for PVI-A, as well as $HFM_{M2\_PVI-B}(P2)$, $HAM_{\%\_M2\_PVI-B}(P2)$ and $\underline{Y}_{\%M2_{PVI}-B}^{h,H}(P2)$, and $HFM_{M3\_PVI-B}(P2)$, $HAM_{\%\_M3\_PVI-B}(P2)$ and $\underline{Y}_{M3_{PVI-B}}^{h,H}(P2)$ for PVI-B.

The *modification-based aggregate* HFMs and corresponding HAM elements are again marked with the additional subscript "Agg", this time corresponding to the two following types of *modification-based* aggregate HFMs obtained by:

1. Summing-up Y-elements of two individual modification-based HFMs related to modification M2 for PVI-A and PVI-B, operating at powers P1 and P2, denoted as "M2" values: $HFM_{Agg\_M2}(P1\&P2)$, $HAM_{\%\_Agg\_M2}(P1\&P2)$ and $\underline{Y}_{\%\_Agg\_M2}^{h,H}(P1\&P2)$, and

2. Summing-up Y-elements of two individual modification-based HFMs related to modification M3 for PVI-A and PVI-B, operating at powers P1 and P2, denoted as "M3" values: $HFM_{Agg\_M3}(P1\&P2)$, $HAM_{\%\_Agg\_M3}(P1\&P2)$ and $\underline{Y}_{\%\_Agg\_M3}^{h,H}(P1\&P2)$.

The calculation (summing-up) of $HAM_{\%\_Agg\_M2}(P1\&P2)$ elements from $HAM_{\%\_M2\_PVI-A}(P1)$ and $HAM_{\%\_M2\_PVI-B}(P2)$ is performed using:

$$\underline{Y}_{\%\_Agg\_M2}^{h,H}(P1\&P2)\frac{\overline{I}_{Tot}^{1}(P1\&P2)}{\overline{V}^{1}} =$$
$$= \underline{Y}_{\%\_M2\_PVI-A}^{h,H}(P1)\frac{\overline{I}_A^1(P1)}{\overline{V}^1} + \underline{Y}_{\%\_M2\_PVI-B}^{h,H}(P2)\frac{\overline{I}_B^1(P2)}{\overline{V}^1} \quad (2)$$

while calculation (summing-up) of $HAM_{\%\_Agg\_M3}(P1\&P2)$ elements from $HAM_{\%\_M3\_PVI-A}(P1)$ and $HAM_{\%\_M3\_PVI-B}(P2)$ is performed using:

$$\underline{Y}_{\%\_Agg\_M3}^{h,H}(P1\&P2)\frac{\overline{I}_{Tot}^{1}(P1\&P2)}{\overline{V}^{1}} =$$
$$= \underline{Y}_{\%\_M3\_PVI-A}^{h,H}(P1)\frac{\overline{I}_A^1(P1)}{\overline{V}^1} + \underline{Y}_{\%\_M3\_PVI-B}^{h,H}(P2)\frac{\overline{I}_B^1(P2)}{\overline{V}^1} \quad (3)$$

where again absolute values are calculated from normalized values using the corresponding fundamental currents.

C. One Fixed-Power Measurement-Based Aggregate HFM

An additional case is introduced to check the errors when only one measurement-based aggregate HFM, obtained for the fixed operating powers of two individually measured PVIs, is used for representing power-dependent changes of their aggregate harmonic characteristics. Although any pair of operating power levels can be used for this comparison, in this paper PVI-A and PVI-B are adjusted to both operate at 50% of their rated powers, i.e. at the middle of their operating ranges. The corresponding *measurement based aggregate* HFM is obtained by summing-up individual HAMs of PVI-A and PVI-B, and is denoted as "M4": $HFM_{Agg\_M4}(50\&50)$, $HAM_{\%\_Agg\_M4}(50\&50)$ and $\underline{Y}_{\%Agg_{M4}}^{h,H}(50\&50)$. This HFM corresponds to one of measurement-based aggregate HFMs already available from "M1" aggregate HFMs (Case 50&50).

III. COMPARISON OF DIFFERENT AGGREGATE HFMs

This section compares results for five different aggregate HFM_{Agg}, denoted as "Ma", "M1", "M2", "M3" and "M4" based on the nomenclature described in the previous section. The reference model is HFM_{Agg_Ma}, i.e. aggregate HFM obtained in direct measurements of two parallel-connected PVIs operating at specific combination of powers.

A. Comparison of Magnitudes of $HAM_{\%\_Agg}$ Elements

The comparison of five different $HAM_{\%\_Agg}(P1\&P2)$ is performed for only diagonal elements, $\underline{Y}_{\%\_Agg}^{h,H}(P1\&P2)$, $h=H$, as off-diagonal elements are small. The results are illustrated in Fig. 2, where up to a five-fold increase in values of $HAM_{\%\_Agg}$ elements can be observed when parallel-connected PVIs transfer from medium operating powers (Case 50&50) to very low operating powers (Case 10&10).

a) Case 10&10 (P1=P2=10% of P_{rated})

b) Case 10&50 (P1=10% and P2=50% of P_{rated})

c) Case 50&10 (P1=50% and P2=10% of P_{rated})

d) Case 50&50 (P1=P2=50% of P_{rated})
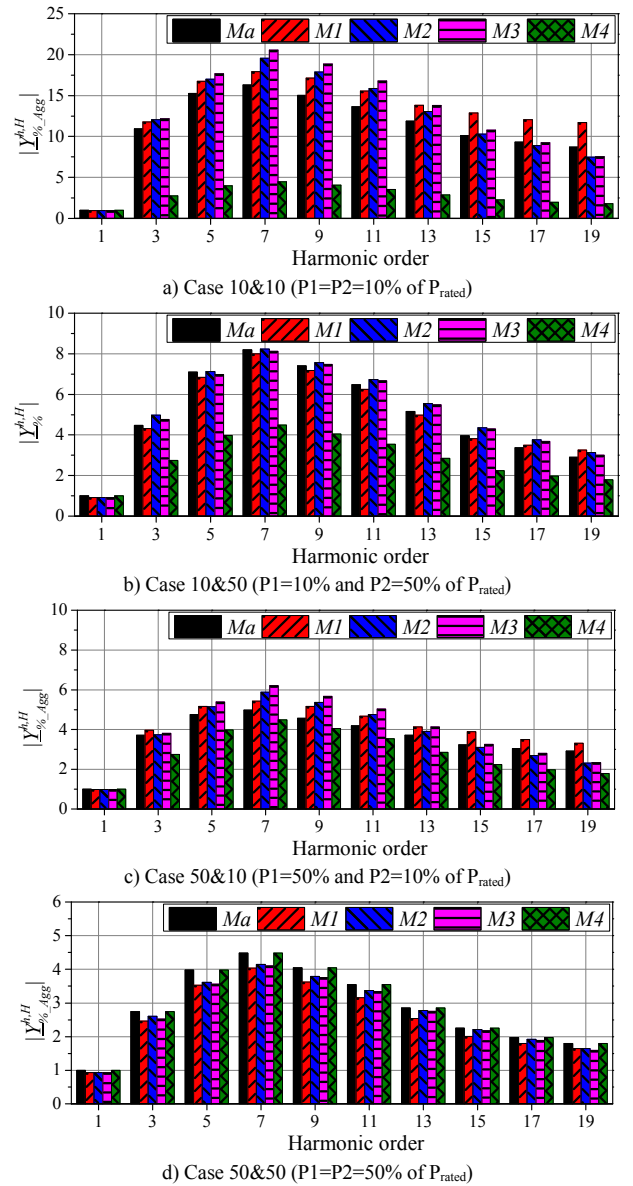
Fig. 2. Power-dependency of diagonal elements of different $HAM_{\%\_Agg}$.

B. *Relative Differences of* $HAM_{\%\_Agg}$ *Elements*

In order to assess the accuracy of the different aggregate HFMs, the 95th percentile values of the relative differences between the $HAM_{\%\_Agg}(P1\&P2)$ elements for models "M1", "M2","M3" and "M4" and "Ma" model values (obtained in direct measurements with parallel-connected PVIs) are calculated with (4), (5), (6) and (7), respectively, and listed in Table II.

$$DIFF_{95th\_M1}(P1\&P2) =$$
$$= (\frac{|Y_{\%\_Agg\_Ma}^{h,H}(P1\&P2) - Y_{\%\_Agg\_M1}^{h,H}(P1\&P2)|}{\Sigma_{H=1}^{n}\Sigma_{h=1}^{n}|Y_{\%\_Agg\_Ma}^{h,H}(P1\&P2)|})_{95th} \times 100\% \quad (4)$$

$$DIFF_{95th\_M2}(P1\&P2) =$$
$$= (\frac{|Y_{\%\_Agg\_Ma}^{h,H}(P1\&P2) - Y_{\%\_Agg\_M2}^{h,H}(P1\&P2)|}{\Sigma_{H=1}^{n}\Sigma_{h=1}^{n}|Y_{\%\_Agg\_Ma}^{h,H}(P1\&P2)|})_{95th} \times 100\% \quad (5)$$

$$DIFF_{95th\_M3}(P1\&P2) =$$
$$= (\frac{|Y_{\%\_Agg\_Ma}^{h,H}(P1\&P2) - Y_{\%\_Agg\_M3}^{h,H}(P1\&P2)|}{\Sigma_{H=1}^{n}\Sigma_{h=1}^{n}|Y_{\%\_Agg\_Ma}^{h,H}(P1\&P2)|})_{95th} \times 100\% \quad (6)$$

$$DIFF_{95th\_M4}(P1\&P2) =$$
$$= (\frac{|Y_{\%\_Agg\_Ma}^{h,H}(P1\&P2) - Y_{\%\_Agg\_M4}^{h,H}(P1\&P2)|}{\Sigma_{H=1}^{n}\Sigma_{h=1}^{n}|Y_{\%\_Agg\_Ma}^{h,H}(P1\&P2)|})_{95th} \times 100\% \quad (7)$$

TABLE II.   THE 95TH PERCENTILE VALUES OF RELATIVE DIFFERENCES
BETWEEN M1-M4 $HAM_{\%\_Agg}$ ELEMENTS AND MA $HAM_{\%\_Agg.}$ ELEMENTS

Case	$DIFF_{95th\_M1}(P1\&P2)$, $DIFF_{95th\_M2}(P1\&P2)$, $DIFF_{95th\_M3}(P1\&P2)$ and $DIFF_{95th\_M4}(P1\&P2)$ in %			
	M1	M2	M3	M4
Case 10&10	2.51	2.87	3.57	6.01
Case 10&50	0.92	0.65	0.50	2.81
Case 50&10	1.40	2.97	3.54	2.28
Case 50&50	0.77	0.77	0.96	0

IV.   TIME- AND FREQUENCY-DOMAIN VALIDATION

This section provides the results of the comparisons of all considered aggregate HFM_{Agg} in both time-domain (by comparing the reconstructed instantaneous current waveforms with the measured ones) and in frequency-domain (by comparing the calculated harmonic magnitudes and phase angles with the measured ones).

A. *Comparison of Time-Domain Current Waveforms*

This section compares reconstructed instantaneous current waveforms with measured instantaneous current waveforms for two parallel-connected PVIs operating at different powers and supplied with voltage waveforms WF2 and WF3 (Part 1 paper provides description of used waveforms). The notation is following nomenclature from Part 1 paper and descriptions from Section II of this paper: measured instantaneous voltage waveforms, *v(t)*, and instantaneous current waveforms, *i(t)*, and related $THDS_I$ values are denoted with a subscript "Meas"; *i(t)* and related $THDS_I$ values reconstructed from aggregate HFM obtained in direct measurements with two parallel-connected PVIs operating at corresponding operating

powers are denoted as "Ma"; *i(t)* and related $THDS_I$ values reconstructed from the aggregate HFM obtained by summing-up two individual HAMs, obtained in separate measurements of each PVI operating at corresponding powers, are denoted as "M1"; *i(t)* and related $THDS_I$ values reconstructed from the aggregate HFM obtained by summing-up two individual HAMs, obtained by applying the first modification (i.e. based on only operating powers of PVIs, as described in Part 1 paper) are denoted as "M2"; "; *i(t)* and related $THDS_I$ values reconstructed from the aggregate HFM obtained by summing-up two individual HAMs, obtained by applying the second modification (i.e. based on operating powers and $THDS_I$ values of PVIs, as described in Part 1 paper) are denoted as "M3"; and *i(t)* and related $THDS_I$ values reconstructed from aggregate HFM obtained by summing-up two individual HAMs of both PVIs operating at fixed power of 50% of their rated powers are denoted as "M4".

The results for time-domain comparison are given in Figs. 3-6, demonstrating, as expected, excellent accuracy of measurement-based aggregate HFMs, assuming they are obtained for the correct PVIs operating powers (results for Ma and M1). If, however, measurement-based aggregate HFM is obtained for one fixed operating power of PVIs and used for modelling operation of PVIs at other operating powers (results for M4), this will result in a fixed instantaneous current waveform, which will introduce errors at other powers.

The results in Figs. 3-6 also demonstrate a very good accuracy of modification-based aggregate HFMs, obtained by summing-up the corresponding HAM elements from the two individual HFMs. Further to results in Part 1 paper, this confirms that the proposed approach is not only correct for modelling of aggregated PVIs power-dependent harmonic characteristics, but can also correctly represent overall behavior of aggregated PVIs.
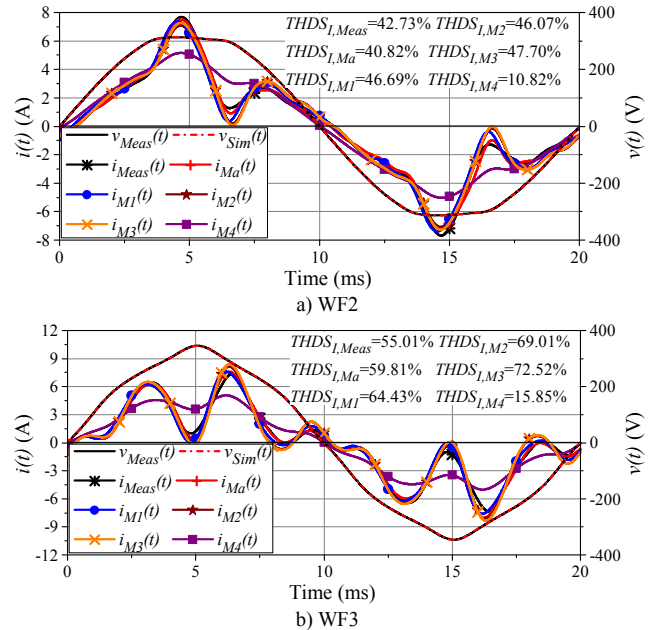
Fig. 3.   Time-domain comparison (Case 10&10).
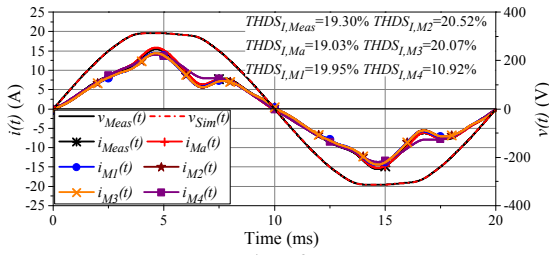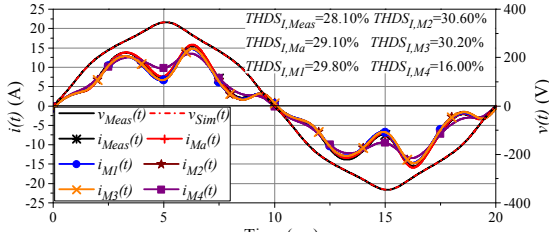
Fig. 4. Time-domain comparison (Case 10&50).
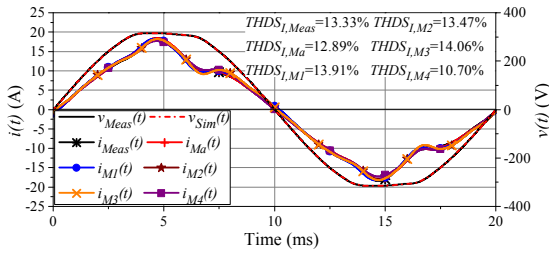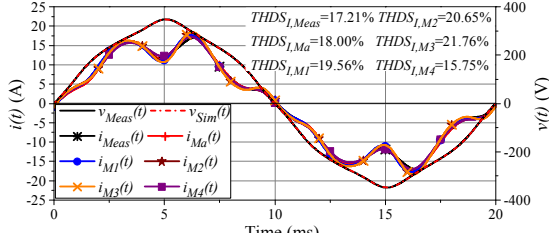
Fig. 5. Time-domain comparison (Case 50&10).
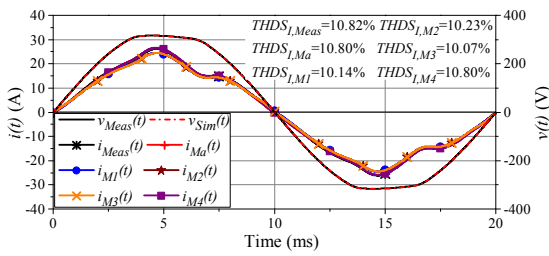
Fig. 6. Time-domain comparison (Case 50&50).

B. Comparison of Frequency-Domain Current Harmonics

This section compares the results for harmonic magnitudes and phase angles obtained by the considered aggregate HFMs with the corresponding measured results obtained for two parallel-connected PVIs operating at different powers and supplied with voltage waveforms WF2 and WF3. These results, shown in Figs. 7-10, confirm conclusions drawn from the time-domain validation.
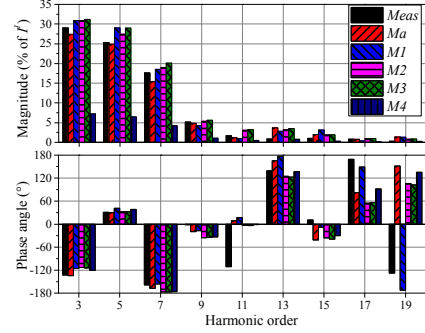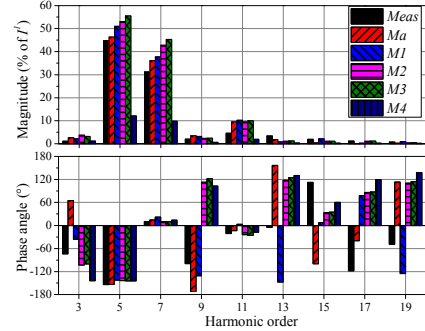
Fig. 7. Frequency-domain comparison (Case 10&10).
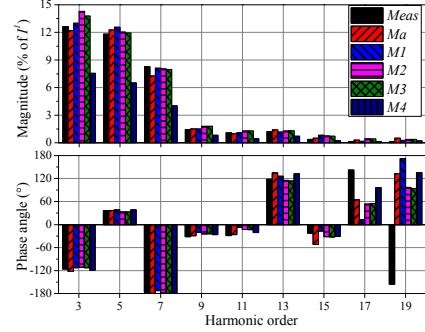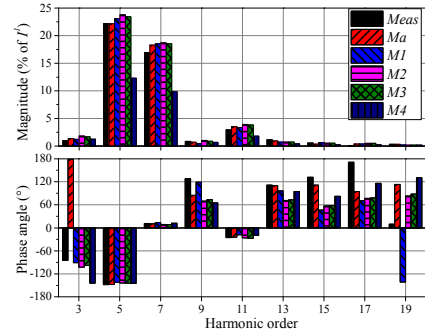
Fig. 8. Frequency-domain comparison (Case 10&50).

a) WF2

b) WF3
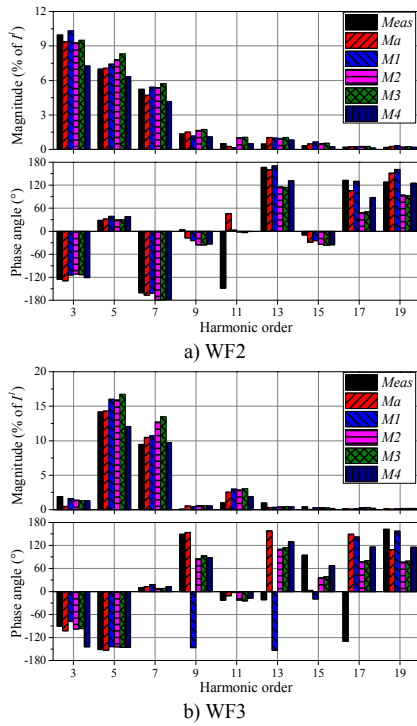
Fig. 9.   Frequency-domain comparison (Case 50&10).

a) WF2

b) WF3
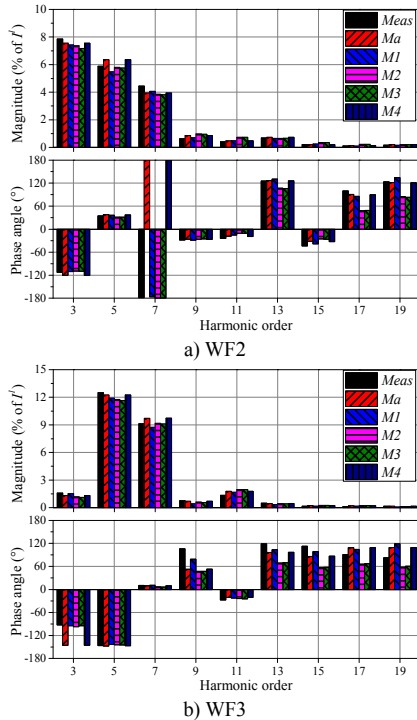
Fig. 10.   Frequency-domain comparison (Case 50&50).

V. CONCLUSIONS

Building on the analysis presented in Part 1 paper [1], this paper evaluates operation of parallel-connected PVI units, investigating whether their correct aggregate HFM can be obtained by summing-up corresponding HAMs of individual HFMs. The paper compares the results for the aggregate HFMs obtained using individual HFMs from measurement-based and two modified HAM approaches, which are illustrated using an example of two parallel-connected PVIs. The main conclusions with reference to the considered case of two parallel-connected PVIs, are:

- Summing-up of HAM elements of individual HFMs seems to be an appropriate way to derive aggregate HFM from individual HFMs, but achieved accuracy of the aggregate HFM depends on how accurate are individual HFMs;

- Measurement-based aggregate HFM, obtained in direct measurements of two parallel-connected PVIs (denoted as "Ma" values), are the most accurate;

- Measurement-based aggregate HFMs, obtained by summing-up HAM elements of two individual PVIs (denoted as "M1" values), require to perform full HFM measurements and obtain individual HFMs for exact (or close) operating powers of two PVIs, as otherwise significant errors might be introduced. This is demonstrated by the errors introduced when $HFM_{Agg\_M4}(50\&50)$ (denoted as "M4") is used to model parallel-connected PVI-A and PVI-B operating at 10% of their rated powers (Case 10&10);

- Two modification-based aggregate HFMs (denoted as "M2" and "M3") provide a very good accuracy with much reduced number of required measurements for deriving individual power-dependent HFMs and, therefore, provide additional benefits for simple and accurate modelling of a large number of parallel-connected PVIs, as they essentially require only information about their operating powers.

REFERENCES

[1] X. Xu, A. Collin, S. Djokic, S. Müller, J. Meyer, J. Myrzik, R. Langella and A. Testa, " Aggregate Harmonic Fingerprint Models of PV Inverters. Part 1: Operation at Different Powers," *18th Int. Conf. on Harm. and Quality of Power (ICHQP)*, Ljubljana, 2018. (submitted)

[2] Dept for Business, Energy & Industrial Strategy, "Solar Photovoltaics Deployment", Part of *Feed-in Tariff Statistics and Energy and Climate Change: Evidence and Analysis Reports*, BEIS, UK, Nov. 2017.

[3] F. Möller, J. Meyer and P. Schegner, "Load Model of Electric Vehicles Chargers for Load Flow and Unbalance Studies," *Electric Power Quality and Supply Reliability Conference (PQ)*, Rakvere, Estonia, 2014.

[4] S. Müller, J. Meyer and P. Schegner, "Characterization of Small Photovoltaic Inverters for Harmonic Modeling," *16th Int. Conf. on Harm. and Quality of Power (ICHQP)*, Bucharest, Romania, 2014.

[5] S. Müller, J. Meyer, P. Schegner and S. Djokic, "Harmonic Modeling of Electric Vehicle Chargers in Frequency Domain," *Int. Conf. on Renewable Energies and Power Quality (ICREPQ)*, La Coruña, Spain, 2015.